

Fig. S1. Immunostaining and mRNA expression in heart tissue and isolated ECs and CMs from *Cd36*^{flox/flox}, EC- *Cd36*^{-/-}, and CM-*Cd36*^{-/-} mice. (A) Sub-organ CD36 mRNA levels in isolated fractionation of female mouse hearts. Data are mean ratios normalized to CM-*Cd36*^{-/-} (set as 1.0). ^δP < 0.0001 versus CM-*Cd36*^{-/-} mice. (B) In situ identified specific CD36 mRNA in heart tissues (arrow). (C-E) mRNA expression in muscle, BAT, and liver of *Cd36*^{flox/flox} and EC- *Cd36*^{-/-} mice. (F) Anti-CD36 antibody stained sections from *Cd36*^{flox/flox}, EC-*Cd36*^{-/-}, and CM-*Cd36*^{-/-} mouse lungs. (G) CM *Cd36* mRNA and protein expressions in *Cd36*^{flox/flox}, EC- *Cd36*^{-/-}, and CM-*Cd36*^{-/-} mouse hearts. (H) qRT-PCR analysis of gene expression in ECs from *Cd36*^{flox/flox} and EC-*Cd36*^{-/-} mice and (I) CMs from EC-*Cd36*^{-/-} mouse hearts.*P < 0.05 and ^δP < 0.0001 versus *Cd36*^{flox/flox} mice. P values were calculated by one-way ANOVA with a Dunnett's multiple comparisons test.

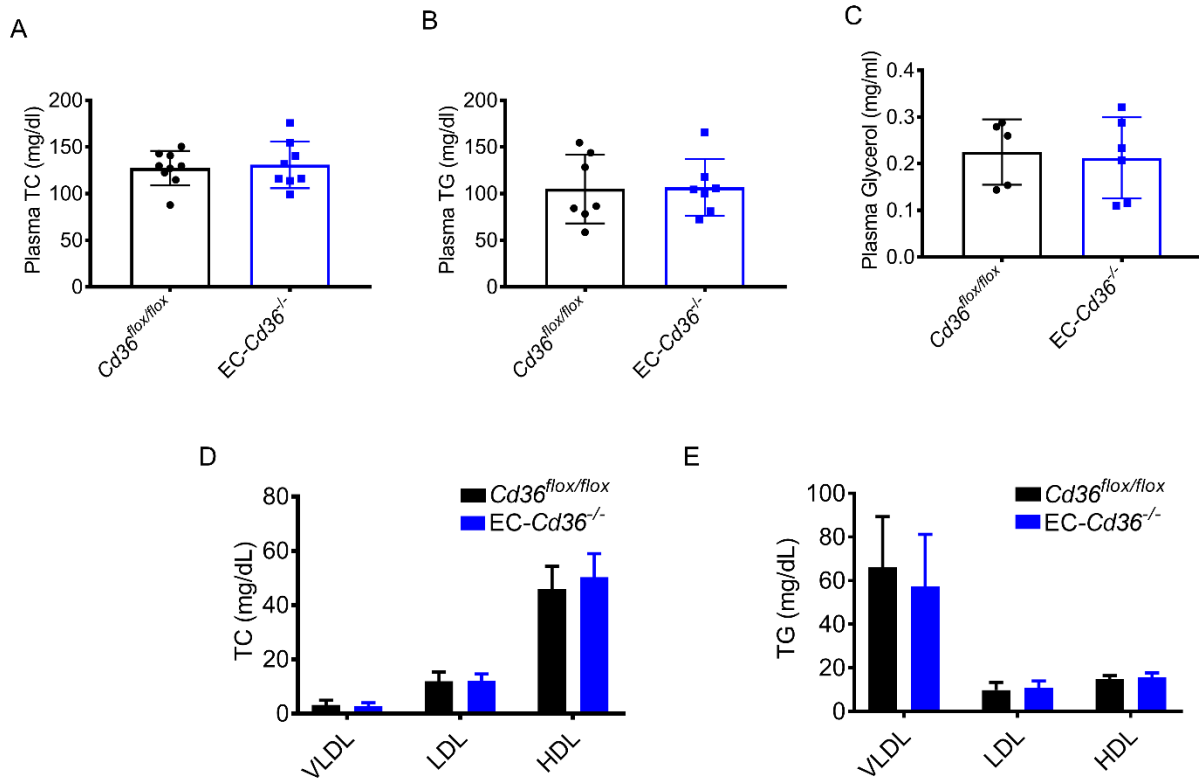


Fig. S2. Plasma lipids, glycerol, and lipoprotein particles in 4-month-old $EC-Cd36^{-/-}$ male mice fed chow diet. (A) Plasma TC and (B) TG levels in $Cd36^{flox/flox}$ and $EC-Cd36^{-/-}$, and $CM-Cd36^{-/-}$ male mice. (C) Plasma glycerol in $EC-Cd36^{-/-}$ mice. (D) TC and (E) TG levels of plasma lipoprotein particles. Data are means \pm S.D. (n=5-8). P values were calculated by one-way ANOVA with a Dunnett's multiple comparisons test.

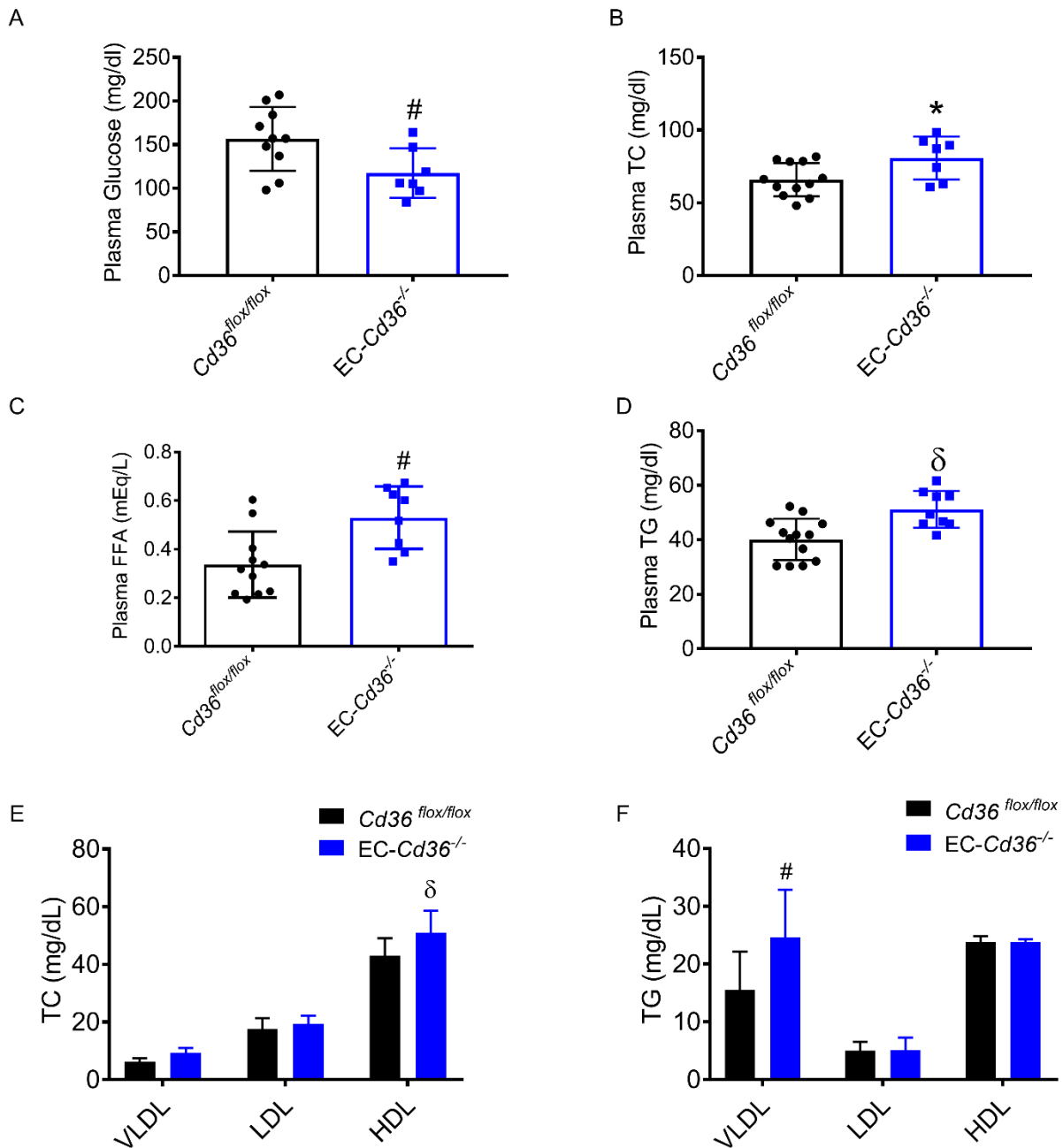


Fig. S3. Increase of plasma glucose, lipids, and lipoprotein particles in 4-month-old EC-*Cd36*^{-/-} female mice fed chow diet. (A) Plasma glucose (B) TC, (C) FFA, and (D) TG. (E) TC and (F) TG levels of plasma lipoprotein particles. Data are means ± S.D (n=8-10). #P < 0.01 and §P < 0.001 compared to *Cd36*^{flox/flox} mice. P values were calculated by one-way ANOVA with a Dunnett's multiple comparisons test.

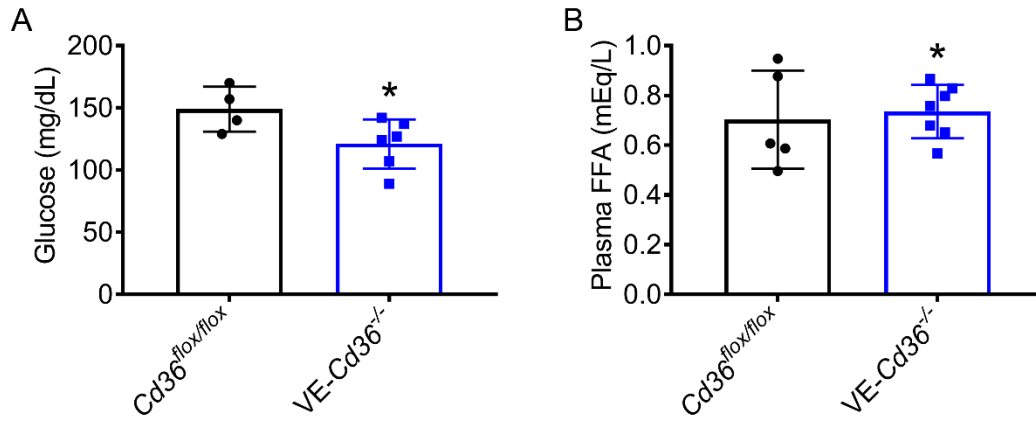


Fig. S4. Decrease of plasma glucose and increase of plasma TC in *VE-Cd36^{-/-}* male mice. (A) Plasma glucose and (B) FFA in *VE-Cd36^{-/-}* male mice. Data are means \pm S.D. (n=4-7). *P < 0.05 compared to *Cd36^{flox/flox}* mice. P values were calculated by one-way ANOVA with a Dunnett's multiple comparisons test.

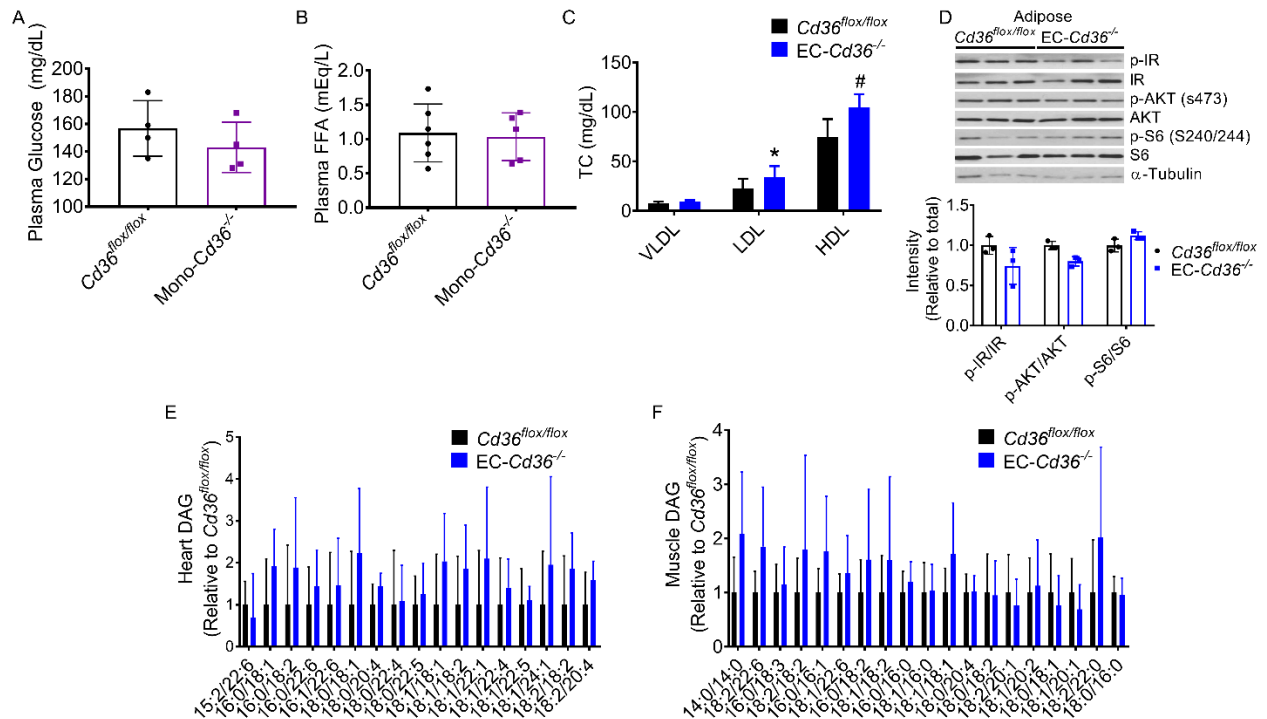


Fig. S5. Plasma and tissue lipids (A) Plasma glucose (n=4) and (B) FFA (n=5-6) in *Mono-Cd36^{-/-}* mice (mRNA decreased 70% compared to *Cd36^{fllox/fllox}* controls) fed chow diet. (C) Plasma lipoprotein TC levels in *EC-Cd36^{-/-}* mice fed 3-week HFD. (D) Western blots (top) and quantification of p-IR, pAKT, and pS6 protein levels (normalized to total IR, Akt, or S6 signal, bottom) from WAT of HFD-fed *Cd36^{fllox/fllox}* and *EC-Cd36^{-/-}* mice. (E) Individual DAG species in the heart (n=4-5) and (F) muscle (n=9-10) of HFD-fed mice. Data are means \pm S.D. * $P < 0.05$ and # $P < 0.01$ compared to *Cd36^{fllox/fllox}* mice. P values were calculated by one-way ANOVA with a Dunnett's multiple comparisons test.

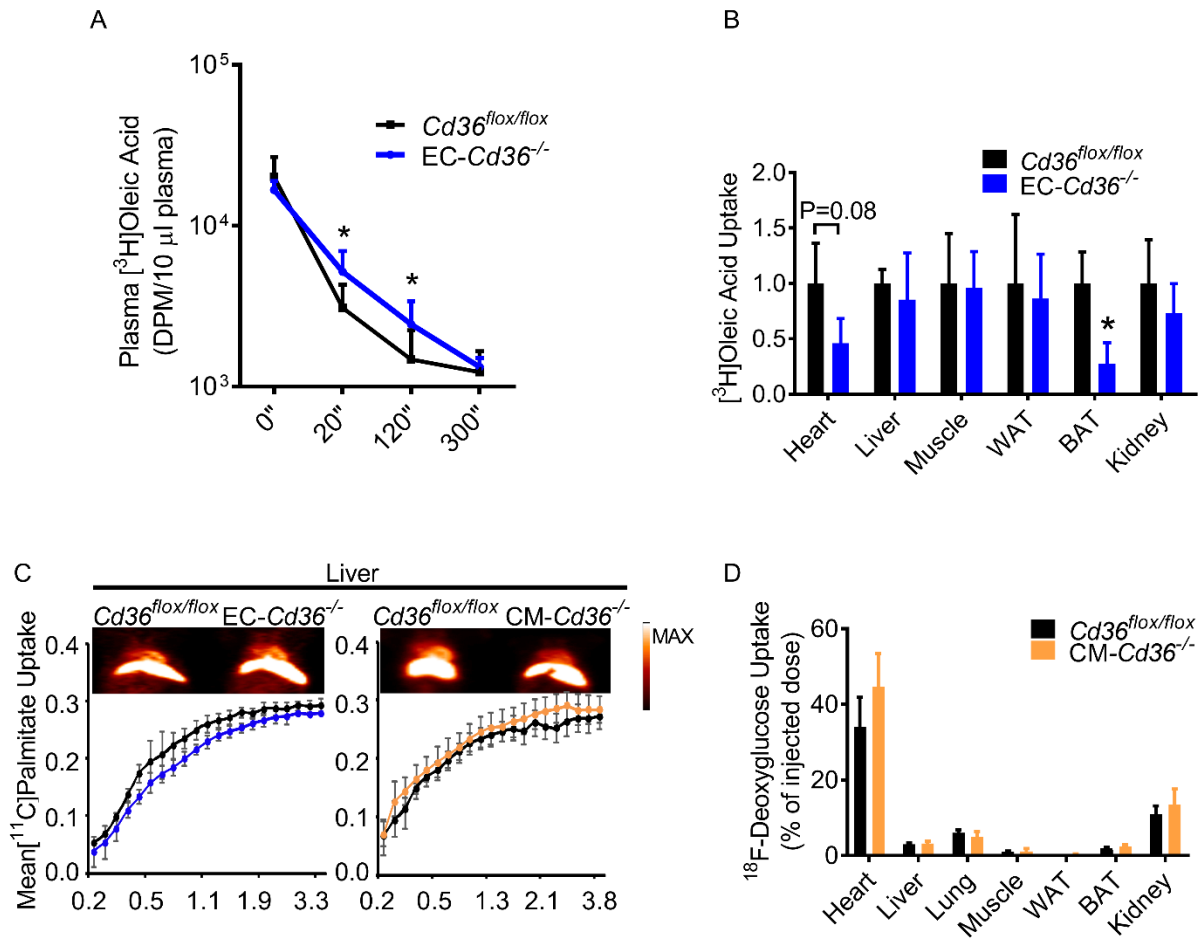


Fig S6. LCFA and [¹⁸F]DG uptake in *EC-Cd36^{-/-}* and *CM-Cd36^{-/-}* mice. (A) 4-5 month old female *Cd36^{flox/flox}* and *EC-Cd36^{-/-}* mice (n=5-6) were fasted for 16 hours; plasma radioactivity (B) their tissue [³H]oleic acid uptake (n=5-6) were measured at shown time points after intravenous injection of [³H]oleic acid and. (C) Real time [¹¹C]palmitic acid uptake into liver of *Cd36^{flox/flox}*, *EC-Cd36^{-/-}*, and *CM-Cd36^{-/-}* mice. Insert shows representative scans of [¹¹C]palmitate uptake at 2 min after tracer administration. (D) [¹⁸F]DG uptake in 4-6 month old *CM-Cd36^{-/-}* male mice. Data are means ± S.D. *P < 0.05 compared to *Cd36^{flox/flox}* controls. P values were calculated by one-way ANOVA with a Dunnett's multiple comparisons test.

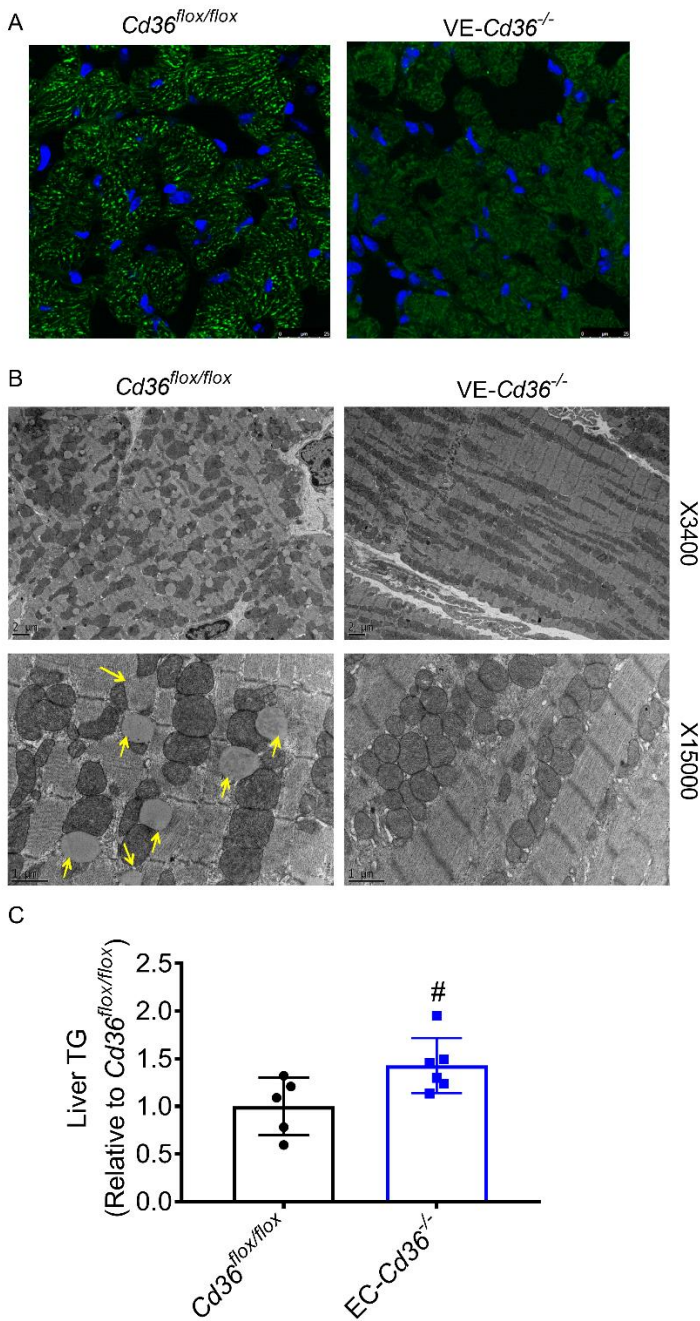


Fig S7. Reduced heart lipid droplet accumulation in VE-*Cd36^{-/-}* mice. (A) BODIPY (493/503) staining of intramuscular lipid droplets in *Cd36^{flx/flx}* and VE-*Cd36^{-/-}* hearts. **(B)** EM images of *Cd36^{flx/flx}* and VE-*Cd36^{-/-}* heart tissues. **(C)** Liver TG content in EC- *Cd36^{-/-}* mice (n=5-6). Data are means \pm S.D. [#]P < 0.01 compared to *Cd36^{flx/flx}* mice. P values were calculated by one-way ANOVA with a Dunnett's multiple comparisons test.

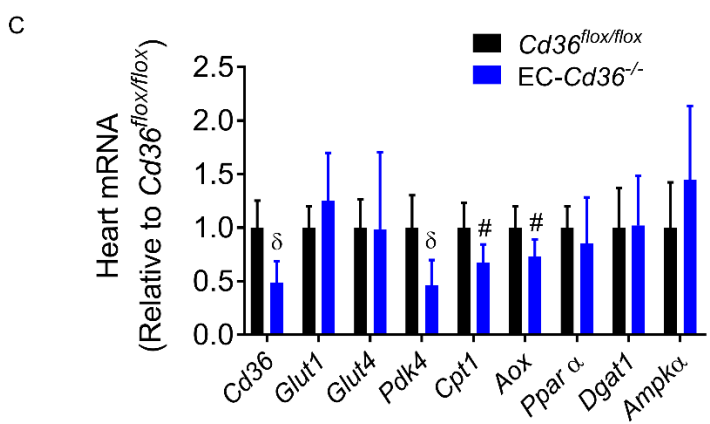
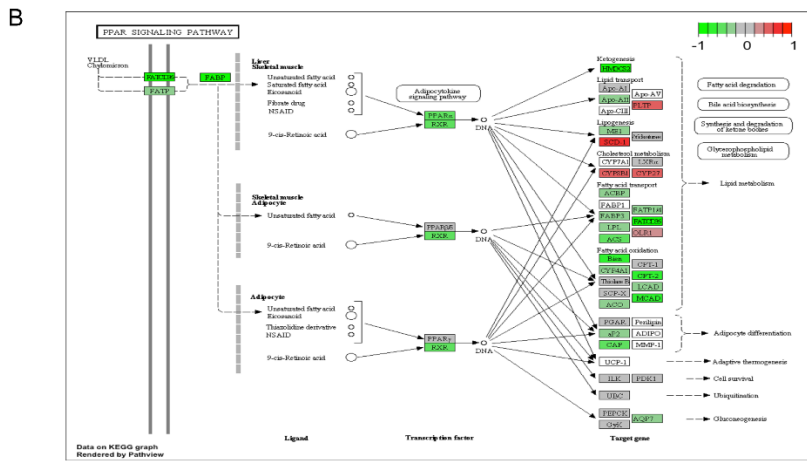
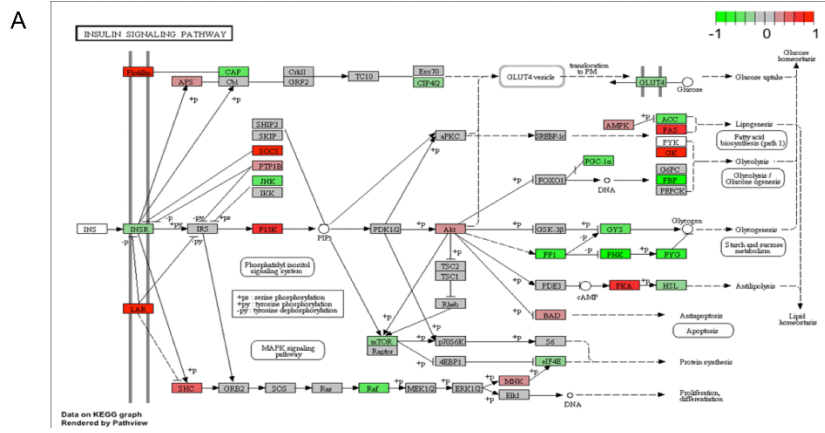


Fig S8. CM- $Cd36^{-/-}$ KEGG analysis and female mouse heart mRNA expression. (A) KEGG analysis of insulin signaling and **(B)** PPAR pathways in CM- $Cd36^{-/-}$ mouse hearts. **(C)** qRT-PCR analysis of mRNA expression in 4-5 month old female $Cd36^{flox/flox}$ and $EC-Cd36^{-/-}$ mice with 16 hours fasting (n=7-9). Data are means \pm S.D. #P < 0.01 and δ P < 0.001 compared to $Cd36^{flox/flox}$ controls. P values were calculated by one-way ANOVA with a Dunnett's multiple comparisons test.

	Primer sequences	Amplification size (base pair)
Primer 1	Sense: 5'-attggcatctgtgtagcgccttggc -3' Antisense: 5'-tgctactatgcactccatgcaggc -3'	WT: 289 bp Cd36 floxed allele: 372 bp
Primer 2	Sense: 5'-attggcatctgtgtagcgccttggc -3' Antisense: 5'-tcaggaccatagcaagtaggc -3'	WT: 2116 bp Cd36 null allele: 420 bp
Primer 3	Sense: 5'-aacactgtgattgtacctg-3' Antisense: 5'-tcaataagcatgtctccgac -3'	WT: 160 bp Cd36 null allele: undetectable

Supplementary Table 1. Primers used for PCR amplification to detect DNA and mRNA from wild type, *Cd36*^{flox/flox}, and *Cd36*^{-/-} mice.